Photooxidation-Induced Changes in Optical, Electrochemical and Photochemical Properties of Humic Substances

Authors

Charles M. Sharpless[a,*]; Michael Aeschbacher[b,c]; Sarah E. Page[c]; Jannis Wenk[c,d,e,f] ; Michael Sander[c]; Kristopher McNeill[c]

Affiliations

[a] Department of Chemistry, University of Mary Washington, USA-22401 Fredericksburg, VA

[b] BMG Engineering AG, CH-8952 Schlieren, Switzerland

[c] Institute of Biogeochemistry and Pollutant Dynamics, ETH Zurich, CH-8092 Zürich, Switzerland

[d] Eawag, Swiss Federal Institute of Aquatic Science and Technology, CH-8600 Dübendorf, Switzerland

[e] Department of Civil & Environmental Engineering, University of California at Berkeley,Berkeley, CA 94720, USA

[f] ReNUWIt Engineering Research Center

* Corresponding author
E-mail: csharple@umw.edu
Phone: +001 540.654.1405
Fax: +001 540.654.1081

Number of pages:	31, with references and figures
Number of figures:	six: five under 3.3” limit (est. 1500 words) one large (est. 600 words)
Number of tables:	none
Number of words:	4,685 in main MS; estimate as 6,785 with figures

Abstract

Three dissolved humic substances (HS), two aquatic fulvic acids and one soil humic acid were irradiated to examine the resulting changes in HS redox and photochemical properties, the relationship between these changes, and their relationship to changes in the optical properties. For all HS, irradiation caused photooxidation as shown by decreasing electron donating capacities. This was accompanied by decreases in specific UV absorbance and increases in the E2/E3 ratio (254 nm absorbance divided by 365 nm). In contrast, photooxidation had little effect on the samples' electron accepting capacities. The coupled changes in optical and redox properties for the different HS suggest that phenols are an important determinant of aquatic HS optical properties and that quinones may play a more important role in soil HS. Apparent quantum yields of H_2O_2, •OH, and triplet HS decreased with photooxidation, thus demonstrating selective destruction of HS photosensitizing chromophores. In contrast, singlet oxygen ($^1O_2$) quantum yields increased, which is ascribed to either decreased $^1O_2$ quenching within the HS microenvironment or the presence of a pool of photostable sensitizers. The photochemical properties show clear trends with SUVA and E2/E3, but the trends differ substantially between aquatic and soil HS. Importantly, photooxidation produces a relationship between the $^1O_2$ quantum yield and E2/E3 that differs distinctly from that observed with untreated HS. This suggests that there may be watershed-specific correlations between HS chemical and optical properties that reflect the dominant processes controlling the HS character.

Introduction

Dissolved organic matter (DOM) is a ubiquitous component of natural surface waters produced by transformation of plant and plankton-derived precursor molecules. It comprises

moderately hydrophobic aromatic polyelectrolytes of variable molecular weight (100's to 1000's of g/mol) (*1,2*) and plays an important role in the biogeochemistry of aquatic environments. For example, microorganisms use DOM as a source of C and N and as an electron shuttle in anaerobic respiration (*3*). DOM also plays important roles in pollutant dynamics, for instance by sorbing organic contaminants and chelating trace and heavy metals (*4,5*). Absorption of sunlight by aromatic chromophores in DOM (*1,6*) leads to formation of reactive oxygen species (ROS) including singlet oxygen ($^1O_2$), hydrogen peroxide (H_2O_2), and hydroxyl radical (•OH) (*7,8*). DOM triplet states ($^3DOM^*$) are both important precursor species for many of these ROS and strong oxidants in DOM-sensitized photoreactions (*7-9*). Together, these photooxidants play a critical role in the redox speciation of trace metals (*10-12*), transformation rates of organic contaminants (*9,13-15*), and solar inactivation of pathogens (*16*).

Absorption of sunlight also leads to DOM photobleaching (destruction of chromophores), photooxidation, and production of low molecular weight organic compounds and inorganic species such as CO and CO_2 (*17-23*). These processes may involve the loss of specific functional moieties and lead to changes in the physicochemical and optical properties of DOM. For example, lignin phenols disappear rapidly in the early stages of photooxidation (*24-26*). Other studies have used FT-ICR-MS and ^{13}C NMR spectroscopy to show that DOM loses aromatic groups during photooxidation (*27,28*). Concomitant changes in DOM optical properties are consistent with a loss of DOM aromaticity (% aromatic C by ^{13}C NMR), including decreases in specific UV absorbance (SUVA, absorbance per mg-C) and fluorescence intensity, and increases in spectral slope and the E2/E3 ratio (ratio of the absorbance at 254 to 365 nm) (*29-35*).

74 The influence of photooxidation on DOM photochemistry remains poorly investigated
75 and understood. Substantial effects seem plausible given that photooxidation changes E2/E3 and
76 SUVA values and that these parameters correlate with quantum yields of $^1O_2$ and CO
77 photoproduction (*36-41*). Zhang *et al.* reported that prolonged irradiation decreased quantum
78 yields for CO production (*38*). To our knowledge, however, no systematic study exists of how
79 irradiation affects photooxidant quantum yields. Cavani *et al.* reported that $^1O_2$ production rates
80 from peat humic acid were unaffected by eight hours of irradiation at 365 nm (*42*). In contrast,
81 Andrews *et al.* reported that H_2O_2 quantum yields for various aquatic samples decreased with
82 increasing irradiation using simulated sunlight (*43*). The results of these two studies are,
83 however, difficult to compare since they not only involve different ROS but also used different
84 samples, methods, irradiation times, and assessment endpoints (i.e., production rates versus
85 quantum yields). Furthermore, the observed trends were not related to the extent of DOM
86 oxidation, which was, until recently, difficult to quantify due to the lack of an appropriate
87 method. The introduction of mediated electrochemical oxidation and reduction (MER and MEO,
88 respectively) now allows reliable quantification of DOM redox state in terms of electron
89 donating and accepting capacities (EDC and EAC) (*44,45*). The EDC and EAC of DOM have
90 been ascribed to phenol and quinone moieties, respectively, which are also chromophores
91 believed to play an important role in DOM photochemistry (*8,9,46-49*).
92 The objective of this study was to systematically investigate the effects of photooxidation
93 on DOM optical, electrochemical and photochemical properties. Studying these changes
94 simultaneously is expected to provide insights into relationships between DOM aromaticity,
95 redox-state, and photoreactivity and to improve understanding of the DOM photobleaching
96 process. Experiments were conducted with three dissolved humic substances (HS): two aquatic

fulvic acids (FAs) and, for contrast, a soil humic acid (HA). Changes in the absorption spectra and apparent quantum yields for the photooxidants $^1O_2$, H_2O_2, •OH, and triplet HS ($^3HS^*$) were measured as a function of irradiation time. The extent of photooxidation was quantified by monitoring changes in EDC and EAC. Spectroscopic data were also used to examine whether correlations between optical and photochemical properties for photooxidized HS are consistent with reported correlations for native DOM isolates (*36*,*37*).

Materials & Methods

Materials. Nordic Aquatic Fulvic Acid (NAFA), Suwannee River Fulvic Acid (SRFA), and Elliot Soil Humic Acid (ESHA) standards were obtained from the International Humic Substances Society (IHSS, www.humicsubstances.org) and used as received. Details for other materials can be found in the *Supporting Information*.

Solutions for Irradiation. All solutions were prepared with Nanopure water (Barnstead) with resistivity >18.2 MΩ cm. The photooxidation experiments were conducted at high HS concentrations (250 mg/L) to ensure the availability of sufficient HS for subsequent analyses. The solutions were prepared by dissolving 25 mg of solid HS isolate in 50 mL of H_2O followed by addition of 1 M NaOH to adjust the pH to 8.0. After pH stabilization (> 30 min), solutions were stirred overnight at room temperature and subsequently diluted to a total volume of 100 mL. The pH was readjusted to 7.0, followed by filtration (0.22 μm) to remove particulate material and sterilize the samples, which were stored for six days at 4 ^oC before use in experiments.

Irradiation Procedure. Aliquots of each HS solution (20 to 25 mL) were transferred to 18 mm diameter quartz tubes containing a magnetic stir bar. The tubes were capped with septa

fitted to allow air sparging of the solutions during irradiation. Sample tubes were placed below the lamp at approximately 30° from horizontal and immersed in a recirculating water bath at 25 °C. A Suntest solar simulator was used at a nominal setting of 700 W m^{-2}. The total photon flux (300 to 700 nm) was $1.4x10^{-4}$ Es L^{-1} s^{-1}, as estimated from *p*-nitroanisole/pyridine actinometry (*50*). Samples were irradiated for a total of 59 h in periods of 11 or 12 h with continuous stirring and sparging with synthetic air. The air bubbles were confined to the center of the sparged solutions and, because the solutions were optically thick, likely had minimal effect on the radiation delivery.

Solution volumes (determined gravimetrically) and pH were measured at the beginning and end of each irradiation period. After each period, small amounts of water were added to replace evaporative losses (always < 0.2 mL) and small volumes of 1 M NaOH were added to re-adjust the pH to 7.0 (the pH never fell below 6.5). At selected intervals, aliquots of solution were removed for analysis and experimentation. To allow for intra-HS redox equilibration, these were stored at 4 °C for at least 3 d before conducting electrochemical and photochemical experiments. All experiments and analyses were conducted within approximately 3 weeks. Duplicate and triplicate photochemical and electrochemical measurements were highly reproducible, indicating that there were no post-irradiation chemical alterations of the HS as detected by our methods.

Optical Properties and Absorbed Energy. Absorbance spectra were collected in 1 cm quartz cuvettes on a Cary 100 spectrophotometer (Varian) using 1 nm slits and phosphate buffer as a blank. Prior to measuring absorbance spectra, HS solutions were diluted in 5 mM phosphate buffer (pH 7.0) by a factor of three (SRFA and NAFA) or ten (ESHA) to ensure that measurements fell into the linear range of the instrument. Optical parameters, including the

E2/E3 ratio and specific UV absorbance at 280 nm ($SUVA_{280}$) were calculated from the measured spectra as detailed in the *Supporting Information*.

Absorption and lamp emission spectra were used to determine the energy absorbed between 300 and 500 nm during irradiation (details in *Supporting Information*). This wavelength range was chosen for its importance to HS photochemistry (*20,34,43,47,51-56*). The conclusions drawn in this study are based on relative changes and change little by setting the long wavelength cutoff to 400 or 450 nm.

Electrochemical Measurements. EDC and EAC values were quantified according to Aeschbacher *et al.* (*44,45,57*) in a glovebox under N_2 (O_2< 0.1ppm; 25±1°C, M. Braun Ltd., Germany). Anoxic buffer solutions were used as described previously (*44,45,57*). HS solutions (3.2 ml of each) from the photooxidation experiments were made anoxic by purging with argon for 20 min prior to transfer to the glovebox. Detailed methods are provided as *Supporting Information*.

Photochemical Experiments. Photooxidant quantum yields were determined using two merry-go-round reactors containing mercury vapor lamps having emission maxima at 365 nm (*58-60*). All quantum yields are therefore reported for excitation at 365 nm. Samples from photooxidation experiments were diluted prior to measuring the production of $^1O_2$, H_2O_2, •OH, and triplet HS ($^3HS^*$). The transient species $^1O_2$, •OH, and $^3HS^*$ were quantified using the probes furfuryl alcohol (FFA), terephthalate (TPA), and 2,4,6-trimethylphenol (TMP), respectively (*36,59,61*). Experimental details and the calculation of apparent quantum yields are provided as *Supporting Information*. Production rates of H_2O_2 were quantified using the Amplex Red assay (Invitrogen) (*62*). Analytical details and quantum yield calculations are provided as *Supporting Information*.

Results and Discussion

Optical Properties. Irradiation caused photobleaching in all the HS. Figure 1 shows the fraction of absorbance remaining and absolute changes in HS absorption coefficients after 59 h (absorption spectra provided as *Supporting Information*). Consistent with previous reports, larger absolute absorbance losses occurred at UV wavelengths, and higher percent losses occurred in the visible. These changes were accompanied by decreases in $SUVA_{280}$ and increases in E2/E3 (Fig. 2) (*29,34,35,63*). Large differences were observed between the soil-derived ESHA and the two aquatic FA in both the magnitude of the optical property changes and the type of changes observed. Specifically, SRFA and NAFA both showed extensive photobleaching (Fig. 1) and clear changes in $SUVA_{280}$ and E2/E3 that were approximately linear with the amount of energy absorbed (Fig. 2). In contrast, much less photobleaching occurred for ESHA even though it absorbed approximately twice the 300 to 500 nm energy (Fig. 1), and the changes in $SUVA_{280}$ and E2/E3 were much smaller and non-linear. These data suggest that ESHA was more resistant than the aquatic FAs to photooxidation. However, it is possible that this difference in resistance was exaggerated by inner-filtering in the ESHA solution. A substantially higher fraction of the energy absorbed by ESHA lay in the visible (ca. 90%) than for the aquatic FAs (ca. 70%), and visible irradiation is known to cause much less efficient photobleaching (*34,35,64*). Thus, the difference between the photobleaching efficiencies for ESHA and the aquatic FAs is probably not as large as implied by these data.

The difference in magnitude of the optical changes notwithstanding, all samples displayed loss of $SUVA_{280}$ and increases in E2/E3 with photobleaching. Both changes indicate loss of aromatic groups (*65,66*) and decreases in molecular weight (*66,67*). Indeed, decreases in molecular weight were observed by size-exclusion chromatography (*Supporting Information*)

189 accompanied by small (ca. 10%) losses of organic-C after 59 h of irradiation (*Supporting*
190 *Information*). The molecular weight dependence of E2/E3 is believed to derive from an
191 increased probability of electronic interactions between chromophores in larger DOM molecules.
192 Specifically, intramolecular charge transfer (CT) complexes involving electron-donating groups
193 (e.g., phenols) and electron-accepting groups (e.g., aromatic ketones and quinones) produces
194 broad, featureless absorbance in the near-UV and visible (i.e., above approximately 370 nm) (*68-*
195 *70*). Thus, observed increases in E2/E3 with irradiation suggest that CT complexes are being
196 destroyed, probably by both decreasing DOM molecular weight and photooxidation of donor
197 and/or acceptor moieties in DOM.

198 *Redox Properties and Relationships to Optical Properties*. In the CT model for DOM
199 optical properties, substituted phenols are suspected electron donors, and aromatic ketones and
200 possibly quinones are suspected acceptors (*68-70*). Phenols and quinones are also major
201 determinants of DOM electrochemical properties. For example, a diverse set of DOM showed a
202 strong correlation between EDC and phenol contents (*44*) (operationally defined as 2x the
203 titrated charge between pH 8 and 10 (*71*)). The EDC of DOM also varies with E_h and pH in
204 ways comparable to low molecular weight phenols (*44*). Finally, the EAC of DOM correlates
205 well with its % aromaticity (*44*), and DOM accepts electrons over a range of reduction potentials
206 consistent with quinones as major electron acceptors (*45*).

207 Figure 3 presents the changes in EDC and EAC with irradiation (values tabulated as
208 *Supporting Information*). The EDC values of all HS samples decreased monotonically with
209 increasing irradiation, with smaller decreases for ESHA that mirror the smaller changes observed
210 in its optical properties compared to the aquatic FAs. To our knowledge, this is the first direct
211 demonstration of DOM photooxidation as quantified by EDC loss. In comparison, all HS

samples showed small changes in EAC. This finding strongly suggests that there was no direct relation between the changes in electron donating and accepting moieties, and, hence, that photooxidation did not convert electron donating phenols and hydroquinones into electron accepting quinone moieties. Instead, the fact that decreases in EDC were not accompanied by similar increases in EAC suggests that photooxidation irreversibly destroyed phenolic moieties. The reason for the small changes in EAC is unknown. They could reflect either a resistance to oxidation by the relevant moieties or a pseudo-steady state resulting from their loss and formation at approximately equal rates.

A comparison of Figs. 2 and 3 shows that the optical properties directly reflect the extent of photooxidation and suggests that the optical properties depend on the amount and nature of redox active moieties. To assess this, we reanalyzed the trends in $SUVA_{280}$ and E2/E3 as a function of EDC and EAC (Figure 4). For the aquatic FAs, $SUVA_{280}$ displays a linear relationship to EDC ($r^2 = 0.904$). For ESHA, there is no apparent relationship, possibly due to the much smaller changes in EDC with irradiation. Stronger correlations of $SUVA_{280}$ with EDC for the aquatic FAs than for soil HA are consistent with prior reports that aromatic-C and EDC are well-correlated for diverse aquatic HS samples but not for different soil-derived HS (*44*). Given that phenolic moieties constitute much more of the aromatic-C in the aquatic FAs than ESHA (*71,72*) (*Supporting Information*), it appears likely that phenols are a major determinant of both EDC and $SUVA_{280}$ in aquatic HS. In contrast, $SUVA_{280}$ appears to vary more with EAC for ESHA (Fig. 4), which could imply that quinones are notable contributors to $SUVA_{280}$ in soil HA. However, this conclusion is tempered by the small and irregular changes in EAC with photooxidation.

To examine the relationship of E2/E3 to EDC and EAC, a larger data set was analyzed that included various untreated aquatic and soil HS (*44*) in addition to the photooxidized samples; missing E2/E3 ratios were measured. For aquatic HS, E2/E3 shows an inverse relationship to EDC, whereas for the soil HA these data are more scattered (Fig. 4). Furthermore, E2/E3 appears to be more sensitive to changes in EDC (steeper slope) for the photooxidized aquatic FAs than for untreated HS isolates. These observations suggest that (i) for aquatic HS, E2/E3 depends strongly on phenol content and (ii) that this dependence is pronounced in samples undergoing photooxidation. For soil HS, on the other hand, E2/E3 seems to be more dependent on EAC (Fig. 4), whereas this relationship is a bit more scattered for aquatic HS, and there is no obvious relationship for the photooxidized FAs. These differences suggest that quinones contribute more to CT absorbance in soil HS than in aquatic HS. Furthermore, in the aquatic FAs undergoing photooxidation, the extent of CT absorbance seems to be independent of quinones. This conclusion is consistent with recent evidence that quinones are not major determinants of CT absorbance in aquatic HS (*46,70*).

Photooxidant Quantum Yields. We further investigated the effect of irradiation on $^1O_2$, H_2O_2, and •OH quantum yields (Φ), defined as the fraction of absorbed photons producing photooxidant. For $^3HS^*$, there is no method to quantify all of the $^3HS^*$ formed. Instead, a proxy for Φ_{3HS*} is used, the quantum yield coefficient, f_{TMP} (M^{-1}), which is the rate constant for TMP loss divided by the rate of light absorption (*61*). Although photochemical reaction rates are sometimes quantified as carbon-normalized rate constants (provided as *Supporting Information*), Φ is a more fundamental parameter with broader general applicability to photochemical modeling. Figure 5 shows how Φ_{1O2}, Φ_{H2O2}, Φ_{OH} and f_{TMP} vary with irradiation. For all HS, the quantum yields of H_2O_2, •OH, and $^3HS^*$ decreased, but, in stark contrast, Φ_{1O2} increased.

257 Attributing physical causes to these trends requires recognition that the quantum yields
258 are "apparent" because they may be affected by a variety of secondary phenomena. For instance,
259 Φ_{H2O2} is a function of the primary quantum yield of O_2^- and the relative rates of uncatalyzed
260 versus HS-catalyzed O_2^- dismutation (*36*). Because uncatalyzed dismutation is apparently the
261 dominant process during SRFA photolysis under conditions similar to those used here (*73*),
262 decreases in Φ_{H2O2} likely reflect lower O_2^- production efficiencies rather than lower dismutation
263 rates. It has recently been suggested that the excited state HS precursor to O_2^- is a long-lived
264 charge-separated species created by electron transfer from singlet excited state donors to ground
265 state acceptor moieties (*74*). The observed EDC loss is consistent with this model, as loss of
266 donors would reduce the yield of charge-separated species and decrease Φ_{H2O2}.

267 In the case of Φ_{OH}, the TPA probe detects both free •OH and other, lower energy
268 hydroxylating species (*59*). Here, we do not distinguish between these hydroxylating species.
269 However, control experiments were conducted with catalase to assess the contribution of H_2O_2-
270 dependent, Fenton-like hydroxylation (*59*). Irradiation did not significantly alter the fraction of
271 hydroxylation occurring through H_2O_2-depedent pathways, which was approximately 50% for
272 ESHA and 20% for SRFA, in good agreement with a previous report (*59*). For NAFA, there was
273 essentially no TPA hydroxylation via H_2O_2. Thus, only a fraction of the decrease in Φ_{OH} can be
274 ascribed to the decrease in Φ_{H2O2}. The remainder must be due to lower quantum yields of
275 excited state oxidants, which are of unknown character, because the mechanism of •OH
276 production by DOM is not established.

277 The parameter used to assess $^3HS^*$ formation, f_{TMP}, depends on both the primary quantum
278 yield of $^3HS^*$ and the rate constant for reaction between $^3HS^*$ and TMP (*61*). Notably, HS do not
279 inhibit TMP oxidation (*58*). Decreases in f_{TMP} thus reflect either a general decrease in $^3HS^*$

280 precursor chromophores or a decrease in a specific $^3HS^*$ pool that reacts rapidly with TMP. In
281 either case, the observed decreases in f_{TMP} indicate that photooxidant production efficiency
282 decreases with irradiation, in agreement with the Φ_{OH} results. For TMP oxidation, the $^3HS^*$
283 precursors are believed to be mainly aromatic ketones and possibly quinones (*46,61*). The
284 present data provide divergent evidence for the role of quinones. For instance, the aquatic FAs
285 have much lower EAC and f_{TMP} than ESHA, consistent with excited state quinones as oxidants of
286 TMP. However, this conclusion does not seem to be compatible with the fact that decreases in
287 f_{TMP} were not paralleled by comparable decreases in EAC.

288 Distinct from the other quantum yields, Φ_{1O2} increased with irradiation. Note that the
289 FFA probe detects $^1O_2$ in the bulk aqueous phase that has escaped the HS microenvironment
290 without being quenched therein (*75*). It is generally accepted that $^1O_2$ is produced by energy
291 transfer from $^3HS^*$ to O_2. Reports by Halladja *et al.* (*76*) and Sharpless (*47*) indicate that a high
292 degree of overlap exists between the $^3HS^*$ pools that produce $^1O_2$ and those that oxidize TMP. If
293 true, a simple way to reconcile the increases in Φ_{1O2} with the decreases in f_{TMP} is to hypothesize
294 that irradiation decreases the efficiency of $^1O_2$ quenching by HS. Thus, even if the yield of $^3HS^*$
295 decreases, higher $^1O_2$ yields could be observed if $^1O_2$ is less effectively quenched within the
296 DOM microenvironment. The loss of EDC is consistent with this hypothesis because quenching
297 of $^1O_2$ by HS probably occurs by an electron transfer mechanism (*77*), which is expected to
298 become less effective as electron donors in HS are destroyed. Also consistent with this view is a
299 recent report that wastewater DOM Φ_{1O2} increases with chemical oxidation by both ozone and
300 chlorine, which destroy electron rich groups selectively and non-selectively, respectively (*41*).
301 An alternative explanation for the increases in Φ_{1O2} is that there may be two classes of $^1O_2$
302 sensitizer (e.g., aromatic ketones and quinones), and that only one of these (Class 1) strongly

303 determines HS optical properties. The destruction of Class 1 sensitizers would decrease
304 absorbance, but the other class of sensitizer would continue producing $^1O_2$. Hence, the results
305 can also be accommodated by a model in which aromatic ketones are Class 1 sensitizers, and
306 quinones are the other Class. This is consistent with negligible EAC loss accompanied by large
307 changes in E2/E3 in the aquatic FAs, where the loss of aromatic ketones would be expected to
308 greatly alter the optical properties (see preceding section) (*46,70*). The hypothesis is also
309 consistent with increasing Φ_{1O2} in the absence of large E2/E3 changes for ESHA; here, quinones
310 may be contributing more to both the photochemical and optical properties (see preceding
311 section) as other sensitizing chromophores are destroyed.

312 *Relationship of* Φ_{H2O2} and Φ_{1O2} *to Optical and Redox Properties*. Previous reports have
313 demonstrated correlations of E2/E3 with Φ_{H2O2} and Φ_{1O2} (*36,37*). Sharpless and co-workers
314 have argued that these originate from the influence of CT interactions on both the optical
315 properties and photochemistry of DOM (*36*). Because photooxidation is an important natural
316 DOM transformation process, we explored whether our results conform to the previously
317 reported correlations. We further investigated relationships between photochemical and
318 electrochemical properties. Figure 6 shows Φ_{1O2} and Φ_{H2O2} as a function of both E2/E3 and
319 EDC for samples undergoing photooxidation. Related plots involving f_{TMP} and Φ_{H2O2} and EAC
320 are provided as *Supporting Information*. We did not construct plots using $SUVA_{280}$, as it
321 correlates inversely and strongly with E2/E3 (*Supporting Information*). Such plots would simply
322 display the reverse of the trends in Figure 6. Although the directions of the trends were the same
323 for all samples, Φ_{H2O2} and Φ_{1O2} vary much more with both E2/E3 and EDC for ESHA than for
324 the aquatic FAs.

Figure 6 also presents the results of Dalrymple *et al.*, who studied HS and DOM isolates (*36*), and Peterson *et al.*, who studied whole water from Lake Superior and its tributaries (*37*). Peterson *et al.*'s results are shown as the reported linear trend because the data include many samples with E2/E3 values well above the range used in Figure 6. For the aquatic FAs undergoing photooxidation, the directions of the trends in Φ_{H2O2} and Φ_{1O2} with E2/E3 agree with previous reports (*36,37*). The Φ_{H2O2} results display good quantitative agreement with those of Dalrymple *et al.* (*36*), suggesting that E2/E3 may be a robust predictor of Φ_{H2O2}. However, Φ_{1O2} is less sensitive to changes in E2/E3 for the photooxidized FAs than for untreated DOM isolates. Notably, the relationship between Φ_{1O2} and E2/E3 for photooxidized FAs resembles that of the Lake Superior samples much more than that of the untreated DOM. This suggests that photobleaching is a major control on DOM optical properties and photochemistry in Lake Superior. Furthermore, it indicates that DOM photooxidation or other dominant DOM degradation processes in particular ecosystems may lead to watershed-specific correlations between optical and photochemical properties.

With EDC, a weak decreasing trend in Φ_{1O2} is observed, while Φ_{H2O2} increases sharply, albeit with different slopes for aquatic HS and soil HS (Fig. 6). The trends can be explained in terms of photophysical concepts expounded previously (*36,47,74*). For example, the decrease in Φ_{1O2} with EDC could reflect lower $^3HS^*$ yields in samples where higher concentrations of electron donating groups engage electron accepting photosensitizers in CT complexes, thus producing absorbance that does not lead to $^3HS^*$ (*36,47*). Conversely, the increase in Φ_{H2O2} with EDC could result from increased formation of charge-separated excited-state precursors to H_2O_2 (*74*) as the content of electron donors increases. As shown in the *Supporting Information*, Φ_{1O2} for the photooxidized FAs and several IHSS aquatic HS and DOM isolates follow similar inverse

relationships to both EDC and EAC, suggesting that DOM with higher concentrations of redox active moieties sensitize $^1O_2$ production less efficiently. This point is also illustrated by plotting Φ_{1O2} versus the total redox activity (EDC + EAC) for all samples in this study plus others for which Φ_{1O2}, EDC, and EAC are available (*Supporting Information*).

Environmental Implications. Aquatic HS have much higher EDC than soil HS, while the opposite is true for EAC (*44*). The present results show that irradiation destroys EDC but alters EAC very little. The lack of EAC creation, even while EDC is destroyed, argues against photochemical oxidation of donor groups to acceptor groups. Rather, the accumulated data point to irreversible oxidation, the target of which may be phenols. Additionally, the photochemical results suggest that aromatic ketones and other possible $^3DOM^*$ precursors such as flavones and chromones are rapidly destroyed by photooxidation.

These results predict a decrease in all photooxidant quantum yields except $^1O_2$ in natural systems where DOM undergoes photooxidation. The direct implication of this finding is that constant quantum yields for HS-derived photooxidants cannot be assumed over the course of days of solar exposure. Based on the energy absorbed in our photooxidation experiments, we estimate that the changes observed here would occur with approximately 240 h of summer solar noon irradiation at 41° N in the upper first cm of a typical inland water (5 mg OC of aquatic DOM from terrestrial sources). However, this estimate is confounded some by uncertainties, such as the extent to which inner-filtering altered the observed photobleaching efficiencies in these experiments and the extent to which storage of our solutions at high concentration for 3 d after irradiation may have fostered intermolecular redox reactions that would not be observed in natural waters. Nonetheless, the contrast between the photochemical trends for photoxidized and untreated HS and DOM (Fig. 6) suggests that variability in photochemical properties of natural

371 waters may arise from multiple processes – mixing of different DOM sources, or photooxidation
372 of a single DOM source – each of which can uniquely alter the optical-photochemical
373 correlations. It is also apparent that compositional differences between aquatic and soil HS lead
374 to very different controls on the optical behavior and hence very different correlations between
375 the optical and photochemical properties. Further efforts to relate the optical and photochemical
376 properties to DOM structure will be needed to provide a sound basis for understanding DOM
377 source-dependent differences in behavior.

378

379 **Acknowledgements**

380 The authors acknowledge Annika Linkhorst for assistance with the spectroscopic measurements,
381 Silvio Canonica and Urs von Gunten for providing facilities and equipment at Eawag, Neil
382 Blough for helpful discussions, and three anonymous reviewers for their insights and comments.

383

384 **Supporting Information Available**

385 Chemicals used, absorption spectra; optical properties; calculations of absorbed energy;
386 electrochemistry details; photochemistry experimental details and calculations; TOC method and
387 results; SEC-OCD results; phenol and aromatic C content of HS; E2/E3 and $SUVA_{280}$
388 relationship to aromaticity; tabulated EDC and EAC; carbon-normalized rates and rate constants
389 for photochemical experiments; f_{TMP} and Φ_{OH} versus E2/E3 and EDC; photooxidant quantum
390 yields versus EAC; correlation between E2/E3 and $SUVA_{280}$; $\Phi_{^1O_2}$ versus EDC and EAC and
391 versus (EDC + EAC)

392

393

394 **References**

1. Thurman, E. M. *Organic Geochemistry of Natural Waters;* Martinus Nijhoff/Junk: Netherlands, 1985.

2. Piccolo, A. The supramolecular structure of soil humic substances: a novel understanding of humus chemistry and implications in soil science. In *Advances in Agronomy (book series);* Sparks, D., Ed.; Academic Press, 2002; Vol. 75.

3. Lovley, D. R.; Coates, J. D.; Blunt-Harris, E. L.; Phillips, E. J. P.; Woodward, J. C. Humic substances as electron acceptors for microbial respiration. *Nature 1996* **1996,** *382,* 445-448.

4. Lu, Y.; Pignatello, J. J. History-dependent sorption in humic acids and a lignite in the context of a polymer model for natural organic matter. *Environ. Sci. Technol.* **2004,** *38,* 5853-5862.

5. Christl, I.; Milne, C. J.; Kinniburgh, D. G.; Kretzschmar, R. Relating ion binding by fulvic and humic acids to chemical composition and molecular size. 2. Metal binding. *Environ. Sci. Technol.* **2001,** *35,* 2512–2517.

6. Brinkmann, T.; Sartorius, D.; Frimmel, F. H. Photobleaching of humic rich dissolved organic matter. *Aquat. Sci.* **2003,** *65,* 415-424.

7. Blough, N. V.; Zepp, R. G. Reactive oxygen species in natural waters. In *In Active Oxygen in Chemistry;* Foote, C. S., Valentine, J. S., Greenberg, A., Liebman, J. F., Eds.; Chapman & Hall, 1995.

8. Richard, C.; Canonica, S. Aquatic phototransformation of organic contaminants induced by coloured dissolved organic matter. In *Handbook of Environmental Chemistry, vol. 2, Part M;* Hutzinger, O., Ed.; Springer-Verlag: Berlin, 2005; p 299−323.

9. Canonica, S. Oxidation of aquatic organic contaminants induced by excited triplet states. *Chimia* **2007,** *61,* 641-644.

10. Sulzberger, B. Effects of light on the biological availability of trace metals. In *Marine Chemistry;* Gianguzza, A., Pelizzetti, E., Sammartano, S., Eds.; Kluwer Academic Publishers, 1997.

11. Voelker, B. M.; Morel, F. M. M.; Sulzberger, B. Iron redox cycling in surface waters: Effects of humic substances and light. *Environ. Sci. Technol.* **1997,** *31,* 1004-1011.

12. Gabarell, M.; Chin, Y.-P.; Hug, S. J.; Sulzberger, B. Role of dissolved organic matter composition on the photoreduction of Cr(VI) to Cr(III) in the presence of iron. *Environ. Sci. Technol.* **2003,** *37,* 4403-4409.

13. Guerard, J. J.; Chin, Y.-P.; Mash, H.; Hadad, C. M. Photochemical fate of sulfadimethoxine in aquaculture waters. *Environ. Sci. Technol.* **2009,** *43,* 8587-8592.

14. Latch, D. E.; Stender, B. L.; Arnold, W. A.; McNeill, K. Photochemical fate of pharmaceuticals in the

environment: cimetidine and ranitidine. *Environ. Sci. Technol.* **2003,** *37,* 3342-3350.

15. Gerecke, A. C.; Canonica, S.; Müller; Sharer, M.; Schwarzenbach, R. P. Quantification of dissolved natural organic matter (DOM) mediated phototransformation of phenylurea herbicides in lakes. *Environ. Sci. Technol.* **2001,** *35,* 3915-3923.

16. Romero, O. C.; Straub, A. P.; Kohn, T.; Nguyen, T. H. Role of temperature and Suwannee River Natural Organic Matter on inactivation kinetics of rotavirus and bacteriophage MS2 by Solar Irradiation. *Environ. Sci. Technol.* **2011,** *45,* 10385-10393.

17. Wetzel, R. G.; Hatcher, P. G.; Bianchi, T. S. Natural photolysis by ultraviolet irradiance of recalcitrant dissolved organic matter to simple substrates for rapid bacterial metabolism. *Limnol. Oceanogr.* **1995,** *40,* 1369-1380.

18. Miller, W. L.; Zepp, R. G. Photochemical production of dissolved inorganic carbon from terrestrial organic matter: significance to the oceanic organic carbon cycle. *Geophys. Res. Lett.* **1995,** *22,* 417-420.

19. Pullin, M. J.; Bertilsson, S.; Goldstone, J. V.; Voelker, B. M. Effects of sunlight and hydroxyl radical on dissolved organic matter: bacterial growth efficiency and production of carboxylic acids and other substrates. *Limnol. Oceanogr.* **2004,** *49,* 2011-2022.

20. White, E. M.; Kieber, D. J.; Sherrard, J.; Miller, W. L.; Mopper, K. Carbon dioxide and carbon monoxide photoproduction quantum yields in the Delaware Estuary. *Mar. Chem.* **2010,** *118,* 11-21.

21. de Bruyn, W. J.; Clark, C. D.; Pagel, L.; Takehara, C. Photochemical production of formaldehyde, acetaldehyde and acetone from chromophoric dissolved organic matter in coastal waters. *J. Photochem. Photobiol. A: Chem.* **2001,** *226,* 16-22.

22. Osburn, C. L.; Wigdahl, C. R.; Fritz, S. C.; Saros, J. E. Dissolved organic matter composition and photoreactivity in prairie lakes of the U.S. Great Plains. *Limnol. Oceanogr.* **2011,** *56,* 2371-2390.

23. Wang, W.; Johnson, C. G.; Takeda, K.; Zafiriou, O. C. Measuring the photochemical production of carbon dioxide from marine dissolved organic matter by pool isotope exchange. *Environ. Sci. Technol.* **2009,** *43,* 8604–8609.

24. Opsahl, S.; Benner, R. Photochemical reactivity of dissolved lignin in river and ocean waters. *Limnol. Oceanogr.* **1998,** *43,* 1297-1304.

25. Scully, N. M.; Maie, N.; Dailey, S. K.; Boyer, J. N.; Jones, R. D.; Jaffé, R. Early diagenesis of plant-derived dissolved organic matter along a wetland, mangrove, estuary ecotone. *Limnol. Oceanogr.* **2004,** *49,* 1667–1678.

26. Spencer, R. G. M.; Stubbins, A.; Hernes, P. J.; Baker, A.; Mopper, K.; Aufdenkampe, A. K.; Dyda, R. Y.; Mwamba, V. L.; Mangangu, A. M.; Wabakanghanzi, J. N.; Six, J. Photochemical degradation of

dissolved organic matter and dissolved lignin phenols from the Congo River. *J. Geophys. Res.* **2009,** *114,* G03010, doi:10.1029/2009JG000968.

27. Stubbins, A.; Spencer, R. G. M.; Chen, H.; Hatcher, P. G.; Mopper, K.; Hernes, P. J.; Mwamba, V. L.; Mangangu, A. M.; Wabakanghanzi, J. N.; Six, J. Illuminated darkness: molecular signatures of Congo River dissolved organic matter and its photochemical alteration as revealed by ultrahigh precision mass spectrometry. *Limnol. Oceanogr.* **2010,** *55,* 1467-1477.

28. Thorn, K. A.; Younger, S. J.; Cox, L. G. Order of functionality loss during photodegradation of aquatic humic substances. *J. Environ. Qual.* **2010,** *39,* 1416-1428.

29. Helms, J. R.; Stubbins, A.; Ritchie, J. D.; Minor, E. C.; Kieber, D. J.; Mopper, K. Absorption spectral slopes and slope ratios as indicators of molecular weight, source, and photobleaching of chromophoric dissolved organic matter. *Limnol. Oceanogr.* **2008,** *53,* 955-969.

30. Hernes, P. J.; Bergamaschi, B. A.; Eckard, R. S.; Spencer, R. M. Fluorescence-based proxies for lignin in freshwater dissolved organic matter. *J. Geophys. Res.* **2009,** *114,* G00F03, doi:10.1029/2009JG000938.

31. Dalzell, B. J.; Minor, E. C.; Mopper, K. M. Photodegradation of estuarine dissolved organic matter: a multi-method assessment of DOM transformation. *Org. Geochem.* **2009,** *40,* 243-257.

32. Kouassi, A. M.; Zika, R. G. Light-induced alteration of the photophysical properties of dissolved organic matter in seawater. Part I. Photoreversible properties of natural water fluorescence. *Neth. J. Sea Res.* **1990,** *27,* 25-32.

33. Lou, T.; Xie, H. Photochemical alteration of the molecular weight of dissolved organic matter. *Chemosphere* **2006,** *65,* 2333-2342.

34. Del Vecchio, R.; Blough, N. V. Photobleaching of chromophoric dissolved organic matter in natural waters: kinetics and modeling. *Mar. Chem.* **2002,** *78,* 231-253.

35. Tzortziou, M.; Osburn, C. L.; Neale, P. J. Photobleaching of dissolved organic material from a tidal marsh-estuarine system of the Chesapeake Bay. *Photochem. Photobiol.* **2007,** *83,* 782-792.

36. Dalrymple, R. M.; Carfagno, A. K.; Sharpless, C. M. Correlations between dissolved organic matter optical properties and quantum yields of singlet oxygen and hydrogen peroxide. *Environ. Sci. Technol.* **2010,** *44,* 5824-5829.

37. Peterson, B.; McNally, A. M.; Cory, R. M.; Thoemke, J. D.; Cotner, J. B.; McNeill, K. Spatial and temporal distribution of singlet oxygen in Lake Superior. *Environ. Sci. Technol.* **2012,** *46,* 7222–7229.

38. Zhang, Y.; Xie, H.; Chen, G. Factors affecting the efficiency of carbon monoxide photoproduction in the St. Lawrence estuarine system (Canada). *Environ. Sci. Technol.* **2006,** *40,* 7771-7777.

39. Xie, H.; Bélanger, S.; Demers, S.; Vincent, W. F.; Papakyriakou, T. N. Photobiogeochemical cycling of carbon monoxide in the southeastern Beaufort Sea in spring and autumn. *Limnol. Oceanogr.* **2009,** *54,* 234–249.

40. Stubbins, A.; Law, C. S.; Uher, G.; Upstill-Goddard, R. C. Carbon monoxide apparent quantum yields and photoproduction in the Tyne estuary. *Biogeosci.* **2011,** *8,* 703–713.

41. Mostafa, S.; Rosario-Ortiz, F. L. Singlet oxygen formation from wastewater organic matter. *Environ. Sci. Technol.* **2013,** *47,* 8179-8186.

42. Cavani, L.; Halladja, S.; Ter Halle, A.; Guyot, G.; Corrado, G.; Ciavatta, C.; Boulkamh, A.; Richard, C. Relationship between photosensitizing and emission properties of peat humic acid fractions obtained by tangential ultrafiltration. *Environ. Sci. Tech.* **2009,** *43,* 4348-4354.

43. Andrews, S. S.; Caron, S.; Zafiriou, O. C. Photochemical oxygen consumption in marine waters: A major sink for colored dissolved organic matter? *Limnol. Oceanogr*. **2000,** *45,* 267-277.

44. Aeschbacher, M.; Graf, C.; Schwarzenbach, R. P.; Sander, M. Antioxidant properties of humic substances. *Environ. Sci. Technol.* **2012,** *46,* 4916-4925.

45. Aeschbacher, M.; Vergari, D.; Schwarzenbach, R. P.; Sander, M. Electrochemical analysis of proton and electron transfer equilibria of the reducible moieties in humic acids. *Environ. Sci. Technol.* **2011,** *44,* 87-93.

46. Golanoski, K.; Fang, S.; Del Vecchio, R.; Blough, N. V. Investigating the mechanism of phenol photooxidation by humic substances. *Environ. Sci. Technol.* **2012,** *46,* 3912-3920.

47. Sharpless, C. M. Lifetimes of triplet dissolved natural organic matter (DOM) and the effect of $NaBH_4$ reduction on singlet oxygen quantum yields: Implications for DOM photophysics. *Environ. Sci. Technol.* **2012,** *46,* 4466-4473.

48. Vaughan, P. P.; Blough, N. V. Photochemical formation of hydroxyl radical by constituents of natural waters. *Environ. Sci. Technol.* **1998,** *32,* 2947-2953.

49. Gan, D.; Jia, M.; Vaughan, P. P.; Falvey, D. E.; Blough, N. V. Aqueous photochemistry of methyl-benzoquinone. *J. Phys. Chem. A* **2008,** *112,* 2803-2812.

50. Dulin, D.; Mill, T. Development and evaluation of sunlight actinometers. *Environ. Sci. Technol.* **1982,** *16,* 815-820.

51. Cooper, W. J.; Zika, R. G. Photochemical formation of hydrogen peroxide in surface and ground waters exposed to sunlight. *Science* **1983,** *220,* 711-712.

52. Haag, W. R.; Hoigné, J.; Gassman, E.; Braun, A. M. Singlet oxygen in surface waters – part II: quantum yields of its production by some natural humic materials as a function of wavelength.

Chemosphere **1984,** *13,* 641-650.

53. Johannessen, S. C.; Miller, W. L. Quantum yield for the photochemical production of dissolved inorganic carbon in seawater. *Mar. Chem.* **2001,** *76,* 271-283.

54. O'Sullivan, D. W.; Neale, P. J.; Coffin, R. B.; Boyd, T. J.; Osburn, C. L. Photochemical production of hydrogen peroxide and methylhydroperoxide in coastal waters. *Mar. Chem.* **2005,** *97,* 14-33.

55. Osburn, C. L.; Retamal, L.; Vincent, W. F. Photoreactivity of chromophoric dissolved organic matter transported by the Mackenzie River to the Beaufort Sea. *Mar. Chem.* **2009,** *115,* 10-20.

56. Paul, A.; Hackbarth, S.; Vogt, R. D.; Röder, B.; Burnison, B. K.; Steinburg, C. E. W. Photogeneration of singlet oxygen by humic substances: comparison of humic substances of aquatic and terrestrial origin. *Photochem. Photobiol. Sci.* **2004,** *3,* 273-280.

57. Aeschbacher, M.; Sander, M.; Schwarzenbach, R. P. Novel electrochemical approach to assess the redox properties of humic substances. *Environ. Sci. Technol.* **2010,** *44,* 87-93.

58. Wenk, J.; von Gunten, U.; Canonica, S. Effect of dissolved organic matter on the transformation of contaminants induced by excited triplet states and the hydroxyl radical. *Environ. Sci. Technol.* **2011,** *45,* 1334-1340.

59. Page, S. E.; Arnold, W. A.; McNeill, K. Assessing the contribution of free hydroxyl radical in organic matter-sensitized photohydroxylation reactions. *Environ. Sci. Technol.* **2011,** *45,* 2818-2825.

60. Wenk, J.; Canonica, S. Phenolic antioxidants inhibit the triplet-induced transformation of anilines and sulfonamide antibiotics in aqueous solution. *Environ. Sci. Technol.* **2012,** *46,* 5455-5462.

61. Canonica, S.; Jans, U.; Stemmler, K.; Hoigné, J. Transformation kinetics of phenols in water: photosensitization by dissolved natural organic material and aromatic ketones. *Environ. Sci. Technol.* **1995,** *29,* 1822-1831.

62. Zhou, M.; Diwu, Z.; Panchuk-Voloshina, N.; Haugland, R. P. A stable nonfluorescent derivative of resorufin for the fluorometric determination of trace hydrogen peroxide: applications in detecting the activity of phagocyte NADPH oxidase and other oxidases. *Anal Biochem.* **1997,** *253,* 162-168.

63. Helms, J. R.; Stubbins, A.; Perdue, E. M.; Green, N. W.; Chen, H.; Mopper, K. Photochemical bleaching of oceanic dissolved organic matter and its effect on absorption spectral slope and fluorescence. *Mar. Chem.* **2013,** *155,* 81-91.

64. Goldstone, J. V.; Del Vecchio, R.; Blough, N. V.; Voelker, B. M. A multicomponent model of chromophoric dissolved organic matter photobleaching. *Photochem. Photobiol.* **2004,** *80,* 52-60.

65. Weishaar, J. L.; Aiken, G. R.; Bergamaschi, B. A.; Fram, M. S.; Fujii, R.; Mopper, K. Evaluation of specific ultraviolet absorption as an indicator of the chemical composition and reactivity of dissolved

organic carbon. *Environ. Sci. Technol.* **2003,** *37,* 4702-4708.

66. Peuravuori, J.; Pihlaja, K. Molecular size distribution and spectroscopic properties of aquatic humic substances. *Anal. Chim. Acta* **1997,** *337,* 133-149.

67. Peuravuori, J.; Pihlaja, K. Preliminary study of lake dissolved organic matter in light of nanoscale supramolecular assembly. *Environ. Sci. Technol.* **2004,** *38,* 5958-5967.

68. Korshin, G. V.; Li, C.-W.; Benjamin, M. M. Monitoring the properties of natural organic matter through UV spectroscopy: a consistent theory. *Wat. Res.* **1997,** *31,* 1787-1795.

69. Del Vecchio, R.; Blough, N. V. On the origin of the optical properties of humic substances. *Environ. Sci.Technol.* **2004,** *38,* 3885-3891.

70. Ma, J.; Del Vecchio, R.; Golanoski, K. S.; Boyle, E. S.; Blough, N. V. Optical properties of humic substances and CDOM: effects of borohydride reduction. *Environ. Sci. Technol.* **2010,** *44,* 5395-5402.

71. Ritchie, J. D.; Perdue, E. M. Proton-binding study of standard and reference fulvic acids, humic acids, and natural organic matter. *Geochim. Cosmochim. Acta* **2003,** *67,* 85-96.

72. Thorn, K. A.; Folan, D. W.; MacCarthy, P. *Characterization of the International Humic Substances Society standard and reference fulvic and humic acids by solution state carbon-13 (^{13}C) and hydrogen-1 (^{1}H) nuclear magnetic resonance spectrometry;* Water-Resources Investigations Report 89-4196; U.S. Geological Survey: Denver, 1989.

73. Garg, S.; Rose, A. L.; Waite, T. D. Photochemical production of superoxide and hydrogen peroxide from natural organic matter. *Geochim. Cosmochim. Acta* **2011,** *75,* 4310-4320.

74. Zhang, Y.; Del Vecchio, R.; Blough, N. V. Investigating the mechanism of hydrogen peroxide photoproduction by humic substances. *Environ. Sci. Technol.* **2012,** *46,* 11836-11843.

75. Latch, D. E.; McNeill, K. Microheterogeneity of singlet oxygen distributions in irradiated humic acid solutions. *Science* **2006,** *311,* 1743-1747.

76. Halladja, S.; ter Halle, A.; Aguer, J.-P.; Boulkamh, A.; Richard, C. Inhibition of humic substances mediated photooxygenation of furfuryl alcohol by 2,4,6-trimethylphenol. Evidence for reactivity of the phenol with humic triplet excited states. *Environ. Sci. Technol.* **2007,** *41,* 6066–6073.

77. Foote, C. S.; Clennan, E. L. Properties and reactions of singlet oxygen. In *Active Oxygen in Chemistry;* Foote, C. S., Valentine, J. S., Greenburg, A., Liebman, J. F., Eds.; Blackie Academic and Professional: Glasgow, 1995.

396

397

Figure Captions

Figure 1: Change in absorbance with irradiation time: (a) $f_{A,59h}$, fraction of absorbance remaining at 59 h; (b) Δa_{59h}, change in absorption at 59 h (base-10 absorption coefficient).

Figure 2: Changes in (a) $SUVA_{280}$ (L mg-C^{-1} m^{-1}) and (b) E2/E3 versus energy absorbed from 300 to 500 nm: (●) SRFA; (◇) NAFA; (▲) ESHA.

Figure 3: Change in EDC and EAC with irradiation time. Samples taken at 0, 11, 35, and 59 h.

Figure 4: $SUVA_{280}$ (L mg-C^{-1} m^{-1}) (top) and E2/E3 (bottom) versus EDC (pH 7, 0.73 V) and EAC (pH 7, -0.49 V): (●) SRFA; (◇) NAFA; (▲) ESHA. For E2/E3, data are also included for IHSS isolates: aquatic (x); soil (○) (redox data from Aeschbacher *et al.* (*44*)).

Figure 5: Changes in photooxidant quantum yields with irradiation time. Error bars represent standard deviation of duplicate or triplicate measurements. (●) SRFA; (◇) NAFA; (▲) ESHA.

Figure 6: Quantum yields of $^1O_2$ and H_2O_2 versus E2/E3 and EDC. (●) SRFA; (◇) NAFA; (▲) ESHA; (■) data from Dalrymple *et al.* (*36*); (---) trend reported by Peterson *et al.* (*37*).

Figure 1

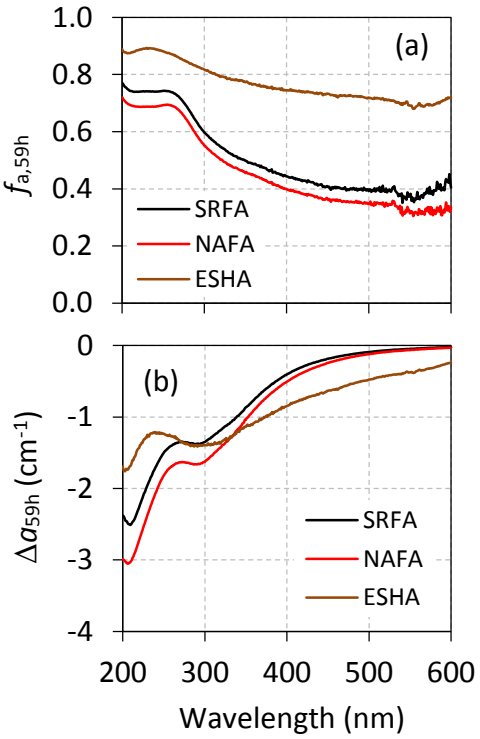
(a)
$f_{a,59h}$
1.0
0.8
0.6
0.4
0.2
0.0
SRFA
NAFA
ESHA
(b)
Δa_{59h} (cm^{-1})
0
-1
-2
-3
-4
200
300
400
500
600
Wavelength (nm)

426 **Figure 2**

427

428

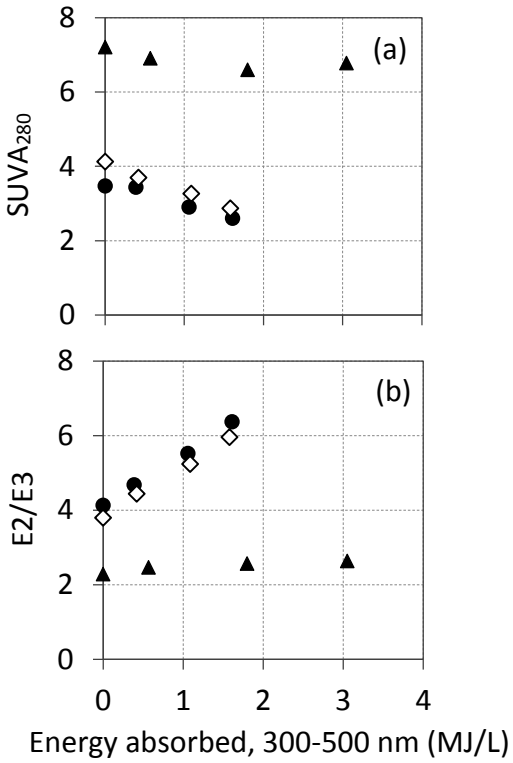

429 **Figure 3**

430

431

432

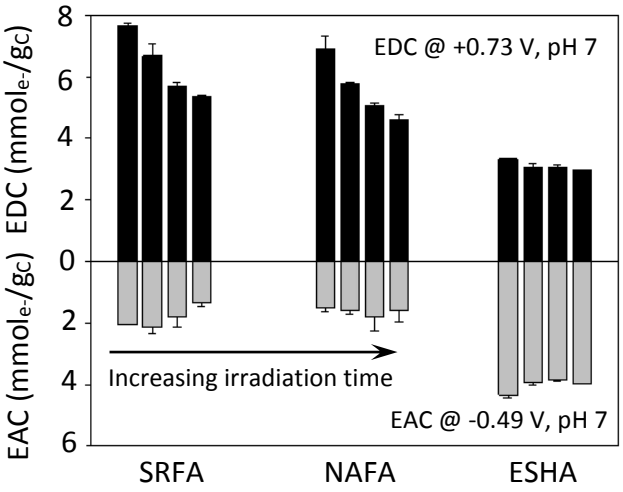

Figure 4

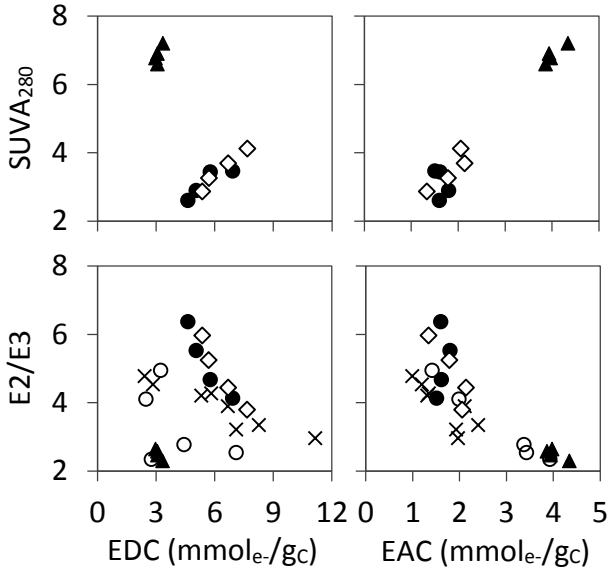

Figure 5

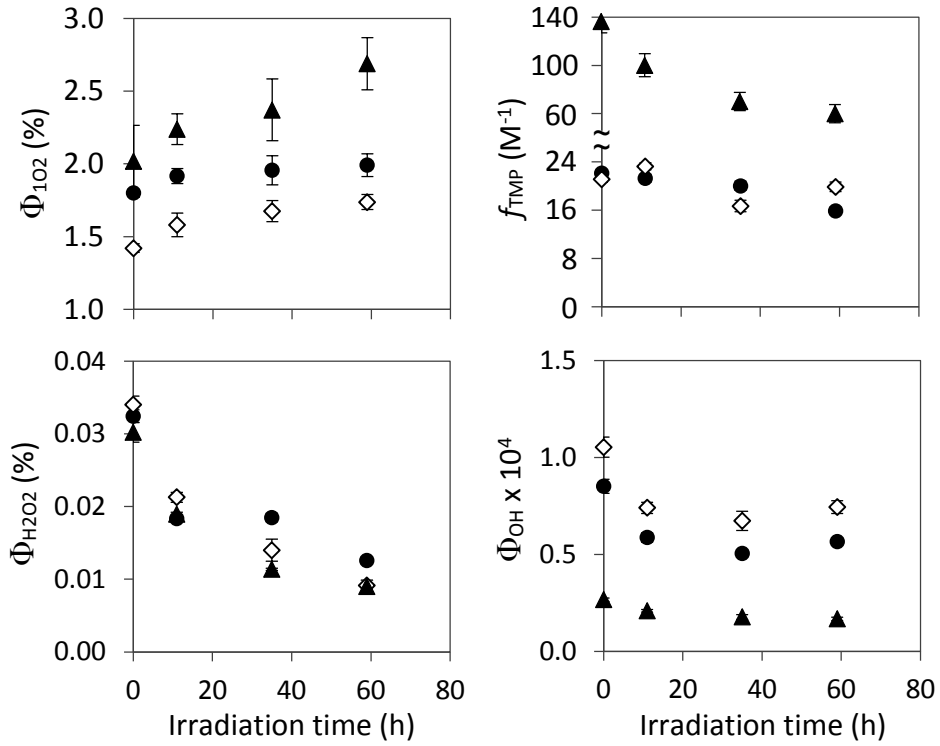
3.0
2.5
2.0
1.5
1.0
Φ_{1O2} (%)
140
100
60
24
16
8
0
f_{TMP} (M^{-1})
0.04
0.03
0.02
0.01
0.00
Φ_{H2O2} (%)
1.5
1.0
0.5
0.0
Φ_{OH} x 10^4
0
20
40
60
80
Irradiation time (h)
Irradiation time (h)

457 **Figure 6**

458

459

460

461

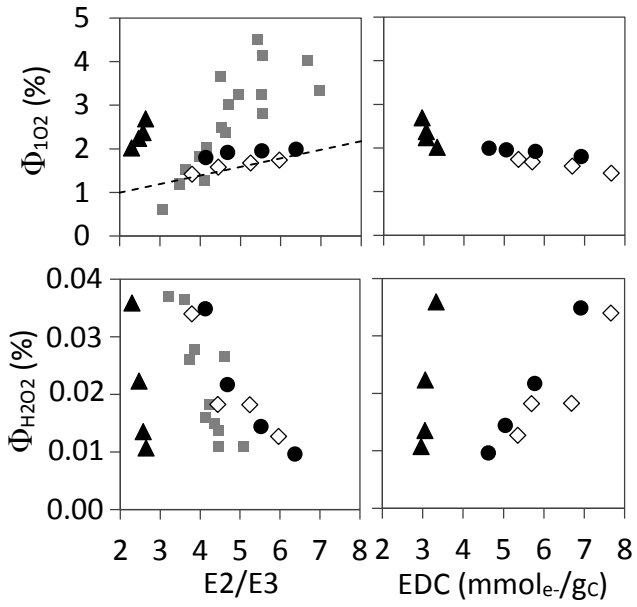

TOC ART

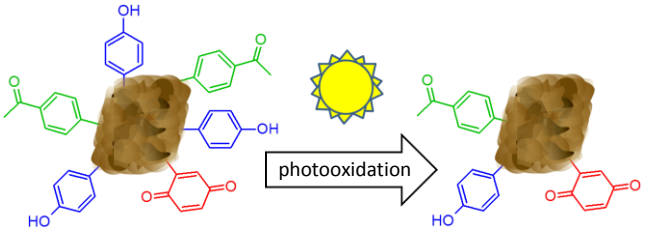

Coupled Changes In

Optical properties
Electrochemical properties
Photooxidant quantum yields